Double-exchange theory of ferroelectric polarization in orthorhombic manganites with twofold periodic magnetic texture

I. V. Solovyev[1,2,*] and S. A. Nikolaev[2]

[1]*Computational Materials Science Unit, National Institute for Materials Science, 1-2-1 Sengen, Tsukuba, Ibaraki 305-0047, Japan*

[2]*Department of Theoretical Physics and Applied Mathematics, Ural Federal University, Mira str. 19, 620002 Ekaterinburg, Russia*

(Received 12 March 2013; published 30 April 2013)

We argue that many aspects of improper ferroelectric (FE) activity in orthorhombic manganites can be rationalized by considering the limit of infinite intra-atomic splitting between majority- and minority-spin states (or the double-exchange limit), which reduces the problem to the analysis of a spinless double-exchange (DE) Hamiltonian. We apply this strategy to the low-energy model, derived from the first-principles electronic-structure calculations, and combine it with the Berry-phase theory of electric polarization. We start with the analysis of the simplest two-orbital model, describing the behavior of the e_g bands, and apply it to the E-type antiferromagnetic (AFM) phase, which in the DE limit effectively breaks up into one-dimensional zigzag chains. We derive an analytical expression for the electronic polarization ($\mathbf{P}^{\rm el}$) and explain how it depends on the orbital ordering and the energy splitting Δ between e_g states. Then, we evaluate parameters of this model for the series of manganites. For these purposes, we start from a more general five-orbital model for all Mn $3d$ bands and construct a new downfolded model for the e_g bands. From the analysis of these parameters, we conclude that the behavior of $\mathbf{P}^{\rm el}$ in realistic manganites always corresponds to the limit of large Δ. This property holds for all considered compounds even in the local-density approximation, which typically underestimates Δ. We further utilize this property in order to derive an analytical expression for $\mathbf{P}^{\rm el}$ in a general twofold periodic magnetic texture, based on the five-orbital model and the perturbation-theory expansion for the Wannier functions in the first order of $1/\Delta$. This expression explains the functional dependence of $\mathbf{P}^{\rm el}$ on the relative directions of spins. Furthermore, it suggests that $\mathbf{P}^{\rm el}$ is related to the asymmetry of transfer integrals, which should have simultaneously symmetric and antisymmetric components in the crystal-field representation. The main contribution to this asymmetry comes from the antiferro-orbital ordering in the $\boldsymbol{ab}$ plane. Finally, we explain how the FE polarization can be switched between orthorhombic $\boldsymbol{a}$ and $\boldsymbol{c}$ directions by inverting the zigzag AFM texture in every second $\boldsymbol{ab}$ plane. We argue that this property is generic and can be realized even in the twofold periodic texture.

DOI: 10.1103/PhysRevB.87.144424 PACS number(s): 75.85.+t, 75.25.−j, 75.47.Lx, 71.15.Mb

I. INTRODUCTION

The multiferroic materials (or multiferroics), where ferroelectricity coexists with some long-range magnetic order, have attracted a great deal of attention.[1] A very special class of multiferroics is improper ferroelectrics. In the latter case, the ferroelectric (FE) polarization not only coexists, but can be induced by the magnetic order. The improper ferroelectrics are expected to display a strong magnetoelectric coupling, which is extremely important for practical applications. For instance, because of such coupling, the FE polarization can be efficiently controlled by the magnetic field, while the magnetization can be controlled by the electric field. From a technological point of view, the ultimate goal is to find materials with the large FE polarization, which would be coupled to the magnetic texture at maximally possible temperature (meaning that the magnetic transition temperature should be also high).

Manganites, crystalizing in the orthorhombic $Pbnm$ and $P2_1nm$ structures, are regarded as one of the key multiferroic materials. Despite low magnetic transition temperature (typically, less than 40 K) and modest values of the FE polarization (less than 1 μC/cm^2), which have been achieved so far,[2] they have all essential ingredients to be called improper ferroelectrics. Namely, the appearance of ferroelectricity coincides with some long range magnetic order. Moreover, the possibility of switching the electric polarization by the magnetic fields has been directly demonstrated experimentally.[3] Therefore, these materials are fundamentally important and are typically used as a playground for testing various theories and models of multiferroicity.

Nevertheless, the theoretical understanding of improper ferroelectricity in these compounds is still rather controversial and there is no unique view on the origin of this effect. First, all multiferroic manganites are rather artificially divided in two groups:

(i) the systems with the twofold periodic E-type antiferromagnetic (AFM) texture (such as $HoMnO_3$ and $YMnO_3$), where the FE activity is attributed to the nonrelativistic exchange striction,[4,5] and

(ii) the rest of the systems, with more general magnetic periodicity, where the FE activity is believed to be due to the relativistic spin-orbit (SO) interaction and the magnetic texture itself is ascribed to the spin spiral.[6–8] The typical example of such systems is $TbMnO_3$, which has nearly fourfold periodic magnetic texture.

This point was rationalized in the previous publications of one of the authors (Refs. 9 and 10), where it was argued that there is no conceptual difference between twofold periodic and other multiferroic manganites. The relativistic SO interaction plays an equally important role in both cases: as it deforms the E-type AFM state in the direction of the spin spiral, it will also deform the spin spiral and form a more general spatially inhomogeneous magnetic state. Thus, the ground state of multiferroic manganites will be neither the collinear E state nor the homogeneous spin spiral. The relativistic

SO interaction is essential for producing this inhomogeneity. However, at least for the considered type of compounds, the FE polarization itself can be regarded as a nonrelativistic quantity in the sense that, for a given inhomogeneous distribution of spins, the appearance of the FE polarization can be described by nonrelativistic theories.

Another group of controversies is related to the interpretation of the origin of FE polarization in manganites, which is frequently done on the basis of rather different standpoints. (i) Most of the model calculations rely on the purely ionic picture, where the noncentrosymmetric distribution of spins gives rise to noncentrosymmetric atomic displacements. Then, the polarization is evaluated in the framework of the point charge model.[4,8,11] Thus, the main assumption is that there is no FE polarization without noncentrosymmetric atomic displacements. (ii) All modern first-principles calculations of the FE polarization are based on the Berry-phase theory.[12,13] Instead of ionic polarization, the Berry-phase theory introduces a more general paradigm of electronic polarization. The latter can be expressed through the Wannier functions and is reduced to the ionic polarization only if the Wannier functions are fully localized at the atomic sites. In this sense, the deviation from the ionic picture is a measure of itineracy of the system. Unlike the ionic term, the electronic polarization can be finite even in centrosymmetric crystalline systems, provided that the inversion symmetry is broken by the magnetic order. Thus, the Berry-phase theory excellently suits for improper ferroelectrics. The first-principles calculations show that the behavior of electronic polarization in manganites can substantially deviate from the ionic picture.[5,14] Nevertheless, most of the model calculations are carried out without resorting to the Berry-phase theory.

The purpose of this work is to make a bridge between first-principles electronic-structure calculations and models of the FE polarization. Our main message is that the Berry-phase theory is the very convenient tool, even in the model calculations. Particularly, in manganites, the behavior of electronic polarization can be described by some "superexchange-type" theories, similar to interatomic magnetic interactions.[15,16] From this point of view, it quite fits the concept of strongly correlated systems, which is typically applied to transition-metal oxides.

Of course, it is not the first attempt to incorporate the Berry-phase theory of electric polarization in the model Hamiltonian approach (see, e.g., Refs. 9,10, and 17–20). Particularly, in their recent work (Ref. 20), Barone *et al.* considered a similar problem: they studied the e_g-electron model for the ferromagnetic (FM) zigzag chain, which describes the properties of the E phase in the double-exchange (DE) approximation, and argued that the onset of the orbital ordering (OO) in the chain gives rise to the electronic polarization. Thus, both specific magnetic backgrounds of the E phase and the OO are indispensable for the FE activity. We agree with this conclusion. Nevertheless, there are at least two points, which surprised us: (i) the functional dependence of electronic polarization, which increases with the Jahn-Teller (JT) and the on-site Coulomb repulsion,[20] although the first-principles calculations show the opposite trend,[5,21] and (ii) we expected that the transfer integrals alone could also contribute to the electronic polarization in the chains. Note that the actual symmetries of manganites ($Pbnm$ or $P2_1nm$) are low and the transfer integrals are noncentrosymmetric. In this work, we will solve this problem analytically. We will argue that the first discrepancy is related to the choice of the reference point for the polarization, which is indeed not unique, while the contribution of the transfer integrals is restricted by the time-reversal symmetry of the DE Hamiltonian.

Our analysis will be based on results of two previous works (Refs. 9 and 10), where (i) a realistic low-energy model for the Mn $3d$ bands of manganites was constructed on the basis of first-principles electronic-structure calculations in the local-density approximation (LDA); (ii) this model was applied for the search of the magnetic ground state; and (iii) the model calculations were supplemented with the Berry-phase theory for the analysis of the FE polarization and its dependence on the form of the magnetic ground state.

In this work, we will further rationalize the story. First, we will show that the behavior of electronic polarization can be well described in the framework of the DE theory.[22,23] The definition of the DE Hamiltonian will be given in Sec. II. Particularly, we will show that with the proper definition of the DE model, which should include effects of orbital polarization of Coulombic origin, one can reproduce, even quantitatively, the values of FE polarization obtained in more general mean-field Hartree-Fock (HF) calculations for the low-energy model. Then, we will introduce an analytically solvable model for the e_g electrons in the zigzag chain (Sec. III A) and argue that, aside from double exchange, the behavior of electronic polarization in realistic manganites always corresponds to the limit of large intra-atomic energy splitting Δ between e_g states (Sec. III B). It will allow us to further generalize our story and derive an analytical expression for the electronic polarization in an arbitrary twofold periodic magnetic texture, based on the perturbation-theory expansion for the Wannier functions in the first order of $1/\Delta$ (Sec. III C). The idea itself has some similarities with the superexchange theory of interatomic magnetic interactions.[15,16] This analytical expression nicely explains the behavior of electronic polarization in the low-energy model as well as in the more general first-principles calculations. It also provides a good quantitative estimate for the polarization. In Sec. III D, we will present a critical analysis of relative directions of electronic and ionic polarizations in the experimental and theoretically optimized $P2_1nm$ structures of $YMnO_3$. Then, in Sec. III E, we will explain how the electronic polarization can be manipulated by changing the magnetic texture. Finally, in Sec. IV, we draw our conclusions.

II. BASIC IDEA AND APPROXIMATIONS

The starting point of our work is that the main electronic and magnetic properties of multiferroic manganites can be described reasonably well by the one-electron Hamiltonian

$$\hat{H}_{ij}^{\mathrm{MF}} = \hat{t}_{ij} + \hat{\mathcal{V}}_i \delta_{ij}, \tag{1}$$

which is constructed in the basis of Wannier orbitals for the Mn $3d$ bands. In this notation, the matrix $\hat{t}_{ij}$ has site-diagonal ($i = j$) and off-diagonal ($i \neq j$) elements: the former describe the crystal-field (CF) effects, while the latter stand for transfer integrals. We do not consider explicitly the relativistic SO interaction. More specifically, it is assumed that the SO

interaction is important for determining the directions of spins in some noncollinear magnetic texture. However, it is unimportant for calculations of the FE polarization itself, provided that the directions of spins are known and specify the form of the one-electron potentials $\hat{\mathcal{V}}_i$. Therefore, the matrix $\hat{t}_{ij}$ does not depend on the spin indices $s(s') = \uparrow$ or $\downarrow$, and can be presented in the form $\hat{t}_{ij} = \|t_{ij}^{mm'}\delta_{ss'}\|$. In the more general five-orbital model, that we consider, the indices m and m' have the following order: $m(m') = xy, yz, 3z^2 - r^2, zx$, and $x^2 - y^2$. In the two-orbital model, constructed only for the e_g bands, the indices m and m' run over $3z^2 - r^2$ and $x^2 - y^2$.

In practice, the electronic low-energy model can be derived from the first-principles electronic-structure calculations, starting from the local-density approximation (LDA).[24] The model can be formulated rather rigorously in the basis of Wannier orbitals for the Mn $3d$ bands. Then, $\hat{t}_{ij}$ is identified with the matrix elements of the LDA Hamiltonian in the Wannier basis. Thus, without $\hat{\mathcal{V}}_i$, the parameters $\hat{t}_{ij}$ are set to reproduce the LDA electronic structure for the Mn $3d$ bands. The parameters of effective Coulomb interactions can be obtained in constraint calculations, combining the random-phase approximation and LDA techniques. Then, the model can be solved in the mean-field HF approximation, which gives us the self-consistent one-electron potentials $\hat{\mathcal{V}}_i$, expressed in terms of effective Coulomb interactions and the density matrices. For details, the reader is referred to Ref. 24.

After the solution, the FE polarization can be obtained by applying the Berry-phase theory.[12,13] Namely, the FE polarization is divided into the ionic (ion) and electronic (el) parts

$$\mathbf{P} = \mathbf{P}^{\text{ion}} + \mathbf{P}^{\text{el}}.$$

The ionic term reflects the noncentrosymmetricity of the crystal structure itself and is associated with the displacements ($\Delta\boldsymbol{\tau}_i$) of ionic charges ($Z_i$) away from the centrosymmetric positions:

$$\mathbf{P}^{\text{ion}} = \frac{1}{V}\sum_i Z_i \Delta\boldsymbol{\tau}_i \tag{2}$$

(V being the primitive cell volume). The electronic term reflects the inversion symmetry breaking in the form of the wave functions, obtained from the solution of quantum-mechanical Schrödinger equations. It can be computed in the reciprocal space by using the formula of King-Smith and Vanderbilt:[12]

$$\mathbf{P}^{\text{el}} = -\frac{ie}{(2\pi)^3}\sum_{n=1}^{M}\int_{\text{BZ}}\langle n\mathbf{k}|\nabla_{\mathbf{k}}|n\mathbf{k}\rangle d\mathbf{k}, \tag{3}$$

where $|n\mathbf{k}\rangle$ is the cell periodic wave function, the summation runs over the occupied bands (n), the $\mathbf{k}$-space integration goes over the first Brillouin zone, and $-e$ ($e > 0$) is the electron charge. In practical calculations, Eq. (3) is replaced by a discrete grid formula.[13] Equation (3) can be also rewritten in terms of the Wannier function (w_n), constructed from $|n\mathbf{k}\rangle$ in the real space:[12]

$$\mathbf{P}^{\text{el}} = -\frac{e}{V}\sum_{n=1}^{M}\int \mathbf{r}|w_n(\mathbf{r})|d\mathbf{r}. \tag{4}$$

In all these equations, it is understood that $\mathbf{P}$ is the *change* of the polarization, obtained in the process of adiabatic lowering of the symmetry.[13] Thus, if the Wannier functions are fully localized at the atomic sites, the electronic term is reduced to the ionic one and, in this sense, there is no conceptual difference between these two contributions. Nevertheless, the electronic polarization gives us more than the ionic term: it incorporates the shift of the Wannier centers from the centrosymmetric atomic positions,[14] which can take place even in the centrosymmetric crystal structure, provided that the inversion symmetry is broken by magnetic or some other electronic degrees of freedom. In practical calculations, all electrons are typically divided in two groups: the contribution of valence electrons is treated by using more general Eq. (3), while the contribution of core electrons is described as $\mathbf{P}^{\text{ion}}$. The same holds in our model analysis: the contribution of the low-energy bands (in our case, the Mn $3d$ bands) is accounted by $\mathbf{P}^{\text{el}}$. Therefore, the contribution of all other occupied states, which are not included to the low-energy model, should be described (at least, approximately) by $\mathbf{P}^{\text{ion}}$. Then, since the oxygen $2p$ band is fully occupied, it is reasonable to take $Z_{\text{O}} = -2e$. On the other hand, all valence states of the rare-earth (RE) ions are empty. This should correspond to $Z_{\text{RE}} = 3e$. In the noncentrosymmetric $P2_1nm$ structure, the Mn sites do not contribute to $\mathbf{P}^{\text{ion}}$.[10] Therefore, the parameter Z_{Mn} is not important for our purposes.

In the previous publications, this procedure was applied to the series of orthorhombic manganites. Particularly, the parameters of the low-energy model, derived from the first-principles calculations, were discussed in Ref. 25. An example of such parameters for $YMnO_3$ can be found in the Supplemental Material of Ref. 10. The properties of the magnetic ground state, obtained from the solution of the low-energy model, and corresponding behavior of the FE polarization were considered in Refs. 9 and 10. Note that a scaling factor was missing in the calculations of the FE polarization reported in Refs. 9 and 18. This error was corrected in Ref. 10.

As far as the FE polarization is concerned, the low-energy model reproduces results of the first-principles electronic-structure calculations (Refs. 5,14, and 21) on a good semiquantitative level. Moreover, the low-energy model was very helpful in clarifying details of the noncollinear magnetic ground state, which can be realized in orthorhombic manganites, namely, (i) the canting of spins and magnetic origin of the twofold periodic phase;[9,10] (ii) the deformation of the spin-spiral texture, yielding FE activity in both twofold and fourfold periodic systems;[9] and (iii) the absence of the magnetic inversion symmetry breaking in systems with odd magnetic periodicity.[9] In this work, we will further rationalize the story by considering the DE limit for the FE polarization.

Let us start with the FM state, where each $\hat{\mathcal{V}}_i$ is diagonal with respect to the spin indices,

$$\hat{\mathcal{V}}_i = \begin{pmatrix} \hat{\mathcal{V}}_i^{\uparrow} & 0 \\ 0 & \hat{\mathcal{V}}_i^{\downarrow} \end{pmatrix},$$

and $\hat{\mathcal{V}}_i^{\uparrow,\downarrow}$ are the 5×5 matrices in the orbital subspace. The states with $s = \uparrow$ are occupied by four electrons and the ones with $s = \downarrow$ are empty. Then, $\hat{\mathcal{V}}_i^{\downarrow}$ can be identically presented in the form $\hat{\mathcal{V}}_i^{\downarrow} = \Delta_{\text{ex}} + \Delta\hat{\mathcal{V}}_i^{\downarrow}$, where Δ_{ex} is the intra-atomic

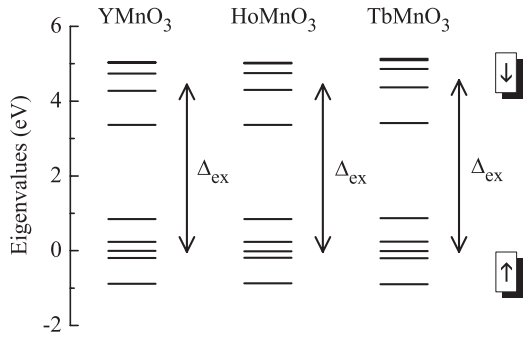

FIG. 1. Eigenvalues of the Hartree-Fock potential, as obtained in the low-energy model for the ferromagnetic phase of $YMnO_3$, $HoMnO_3$, and $TbMnO_3$ (results of Refs. 9 and 10 for the experimental $Pbnm$ structure). Δ_{ex} is the intra-atomic splitting between centers of gravity of the majority- ($\uparrow$) and minority- ($\downarrow$) spin states.

exchange splitting between centers of gravity of the majority- ($\uparrow$) and minority- ($\downarrow$) spin states, and $\Delta\hat{\mathcal{V}}_i^{\downarrow}$ describes the orbital splitting of unoccupied $\downarrow$-spin states. Moreover, four $3d$ electrons obey Hund's first rule, which tend to form the state with the maximal spin $S = 2$. Therefore, aside from on-site Coulomb repulsion (U), Δ_{ex} will include a large contribution $2SJ_H$ proportional to S and the intra-atomic exchange coupling J_H. This is the main reason why for many applications Δ_{ex} can be treated as the largest physical parameter, and the DE limit corresponds to the extreme situation where $\Delta_{ex} \to \infty$.[22,23] On the other hand, the splitting of unoccupied $\downarrow$-spin states is considerably weaker. For example, in the HF approximation, it is caused by relatively small nonsphericity of the Coulomb potential.

Therefore, for $\Delta_{ex} \to \infty$ the details of $\Delta\hat{\mathcal{V}}_i^{\downarrow}$ become unimportant and our first approximation is to replace $\Delta\hat{\mathcal{V}}_i^{\downarrow}$ by $\hat{\mathcal{V}}_i^{\uparrow}$, i.e.,

$$\hat{\mathcal{V}}_i \approx \begin{pmatrix} \hat{\mathcal{V}}_i^{\uparrow} & 0 \\ 0 & \hat{\mathcal{V}}_i^{\uparrow} + \Delta_{ex} \end{pmatrix}. \tag{5}$$

Thus, the spin-dependent part of $\hat{\mathcal{V}}_i$ no longer depends on the orbital indices and can be transformed by means of regular spin rotations.

A typical example, illustrating the structure of the atomic $3d$ level splitting by the Coulomb and exchange potentials in the low-energy model, is shown in Fig. 1. Typical values of Δ_{ex} in manganites are about 4.5 eV, while the splitting of the $\downarrow$-spin states is about 1.7 eV. As we will see below, this difference is sufficient to justify the use of the DE limit for the FE polarization.

As the next step, let us consider an arbitrary magnetic texture, where the direction of spin ($\mathbf{e}_i$) at each site of the lattice is specified by the vector $\mathbf{e}_i = (\cos\phi_i \sin\theta_i, \sin\phi_i \sin\theta_i, \cos\theta_i)$. The corresponding electronic structure is obtained by the unitary transformation of Eq. (5):

$$\hat{\mathcal{V}}_i \to \hat{U}(\theta_i,\phi_i)\hat{\mathcal{V}}_i\hat{U}^{\dagger}(\theta_i,\phi_i), \tag{6}$$

in terms of the spin rotation matrices

$$\hat{U}(\theta_i,\phi_i) = \begin{pmatrix} \cos\frac{\theta_i}{2} & \sin\frac{\theta_i}{2}e^{-i\phi_i} \\ -\sin\frac{\theta_i}{2}e^{i\phi_i} & \cos\frac{\theta_i}{2} \end{pmatrix}.$$

Here, it is assumed that the one-electron potential for an arbitrary direction of spin can be obtained by the rigid spin rotations [Eq. (6)] without additional self-consistency. This is a very good approximation in the case of manganites, because (i) due to the strong Hund's coupling, the local spin magnetization will always tend to stay in the saturated state and only weakly depend on the directions of spins at other magnetic sites. (ii) The orbital configuration is fixed by the JT distortion and practically does not depend on the spin texture. In principle, an orbital reconstruction could additionally minimize the energy of interatomic exchange interactions.[16] However, this reconstruction is penalized by the large energy splitting between two e_g orbitals, which are selected by the JT distortion.[25]

The next step is to transform Eq. (6) to the local coordinate frame, corresponding to the z direction of spin at each site of the lattice. Then, the transfer integrals will transform as

$$\hat{t}_{ij} \to \hat{U}^{\dagger}(\theta_i,\phi_i)\hat{t}_{ij}\hat{U}(\theta_j,\phi_j).$$

Finally, taking the limit $\Delta_{ex} \to \infty$, we obtain the well-known DE Hamiltonian

$$\hat{H}_{ij}^{DE} = \xi_{ij}\hat{t}_{ij} + \hat{\mathcal{V}}_i^{\uparrow}\delta_{ij}, \tag{7}$$

which is formulated in the subspace of $\uparrow$-spin states, in the local coordinate frame,[22,23] and where ξ_{ij} is the $\uparrow\uparrow$ element of $\hat{U}^{\dagger}(\theta_i,\phi_i)\hat{U}(\theta_j,\phi_j)$:

$$\xi_{ij} = \cos\frac{\theta_i}{2}\cos\frac{\theta_j}{2} + \sin\frac{\theta_i}{2}\sin\frac{\theta_j}{2}e^{-(\phi_i-\phi_j)}.$$

Since for the ferromagnetically and antiferromagnetically coupled spins ξ_{ij} is equal to 1 and 0, respectively, any AFM phase in the DE limit effectively breaks up into FM segments. Then, the description of the E-type AFM phase is reduced to the analysis of one-dimensional FM zigzag chains.[4,20]

Next, we investigate the abilities of the DE model for the description of the FE polarization. For these purposes, we diagonalize the DE Hamiltonian [Eq. (7)], and then evaluate the electronic polarization, using the Berry-phase formula [the discrete analog of Eq. (3)].[12,13] This procedure was applied to the series of orthorhombic manganites $TbMnO_3$, $HoMnO_3$, and $YMnO_3$ (and using both experimental and theoretically optimized crystal structure for the latter compound).[9,10] The obtained polarization was compared with results of self-consistent HF calculations for the same low-energy model, but without additional approximations associated with the DE limit [Eq. (1)]. Typical results of such calculations are illustrated in Fig. 2 for the $Pbnm$ phase of $YMnO_3$ (other systems show very similar behavior). More specifically, we consider a twofold periodic magnetic texture, which is explained in Fig. 2(c), and keep the AFM coupling between adjacent planes $z = 0$ and $c/2$, as explained in Fig. 2(a). Then, $\phi = 0^{\circ}$ and 180° correspond to the AFM alignment of the E type, while $\phi = 90^{\circ}$ corresponds to the spin-spiral alignment. For this geometry, $\mathbf{P}^{el}$ should be parallel to the orthorhombic $\boldsymbol{a}$ axis.[5] In the DE model itself, we consider two levels of approximations. In the first case (denoted as "DE LDA"), we neglect $\hat{\mathcal{V}}_i^{\uparrow}$ and consider only the CF splitting and transfer integrals, derived from the LDA band structure. Then, we modulate the transfer integrals with ξ_{ij}. In the second case, we consider the full DE Hamiltonian [Eq. (7)], including $\hat{\mathcal{V}}_i^{\uparrow}$

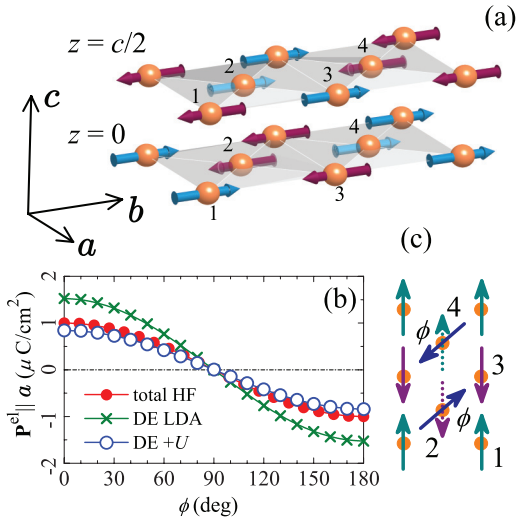

FIG. 2. (Color online) (a) E-type antiferromagnetic texture. (b) Behavior of electronic polarization in $YMnO_3$ upon rotation of magnetic moments, as obtained in the self-consistent mean-field Hartree-Fock approximation (total HF), in the double-exchange model for the LDA band structure (DE LDA), and in the double-exchange model with the Hartree-Fock potential $\hat{\mathcal{V}}_i^{\uparrow}$ (DE + U). In the rotated texture, the directions of spins at the sites 1 and 3 were fixed, while the spins at the sites 2 and 4 were rotated by the angle ϕ, as explained in panel (c). The planes $z = 0$ and $c/2$ were coupled antiferromagnetically.

(denoted as "DE + U"). All magnetic solutions are insulating. Therefore, we can use the Berry-phase formula for the analysis of $\mathbf{P}^{el}$. The DE LDA scheme overestimates the electronic polarization by about 50%. Nevertheless, this is to be expected because LDA underestimates the band gap. Therefore, the FE polarization should be generally larger. Similar behavior was found in the first-principles calculations.[5,21] The analytical expression, explaining the band-gap dependence of $\mathbf{P}^{el}$, will be derived in Sec. III A. The band-gap problem is corrected by $\hat{\mathcal{V}}_i^{\uparrow}$. Therefore, the FE polarization, derived in the DE + U scheme, is smaller. Moreover, results of self-consistent HF calculations are well reproduced by the DE + U scheme: although $\mathbf{P}^{el}$ in the approximate DE + U scheme is systematically smaller, the typical difference, which was obtained for all considered systems, is less than 15%.

This is our main observation and also the main motivation of the rest of our work. By considering the DE limit, we will slightly lose in the accuracy, but instead we will be able to rationalize the problem and derive several analytical expressions for the FE polarization in orthorhombic manganites. Our analysis will also clarify results of the low-energy model and first-principles calculations.

III. RESULTS

We start with the analysis of the E-type AFM phase. As was pointed out above, in the DE limit, the FE AFM E phase breaks up into one-dimensional FM zigzag chains. Therefore, the key moment for understanding the FE activity in the E phase is the analysis of the isolated zigzag chain.[20] In Sec. III A, we start such an analysis with the simplest but analytically solvable model for the e_g electrons. The model is introduced in a rather formal way, as is typically done in model considerations (see, e.g., Ref. 23). Nevertheless, it should be understood that this model can be derived rigorously, along the same lines as it was discussed in Sec. II. In Sec. III B, we will indeed derive parameters of such a model, starting from a more general five-orbital model, which was obtained from the first-principles calculations.[9,10,25] Section III A has two important conclusions. First, we will discuss the choice of the reference point for the analysis of electronic polarization and argue that this choice is not unique. Particularly, it will allow us to reconcile our results with those by Barone *et al.* on a similar model.[20] Second, from the analysis of this model, we will conclude that the situation, realized in most of the electronic-structure calculations (even in ordinary LDA), corresponds to the limit of large energy splitting Δ between atomic e_g states, which incorporates the effects of the JT distortion and (optionally) the on-site Coulomb repulsion. Then, by considering the large-Δ limit, in Sec. III C we will derive an analytical expression for the FE polarization, which is based on the five-orbital model. This expression explains the functional dependence of $\mathbf{P}^{el}$ on the relative directions of spins and the form of nearest-neighbor transfer integrals. In Sec. III D, we will analyze relative directions of electronic and ionic polarizations in the noncentrosymmetric $P2_1nm$ structure and point out the problem of structural optimization, which apparently exists in some of the first-principles calculations, where the directions of noncentrosymmetric atomic displacements are inconsistent with the type of the OO, realized in the FM zigzag chain. In Sec. III E, we consider the possibility of switching the FE polarization by changing the magnetic texture: we argue that, even in the twofold periodic texture, there is another type of the AFM zigzag ordering, which leads to a finite FE polarization parallel to the orthorhombic $\boldsymbol{c}$ axis. However, the value of this polarization is expected to be small.

A. Analytically solvable model for e_g electrons in the zigzag chain

The zigzag chain consists of the two groups of sites: the lower corner sites 1 and the upper corner sites 2 (see Fig. 3). The orthorhombic translation $\boldsymbol{a}$ transforms each group to itself (the translated sites are denoted as $1'$ and $2'$, respectively). It is assumed that the lattice distortion stabilizes some e_g orbitals at the sites 1 and 2, which will be denoted as $|1\rangle_1$ and $|1\rangle_2$, respectively. The orthogonal to them e_g orbitals are denoted as $|2\rangle_1$ and $|2\rangle_2$, respectively. Furthermore, it is assumed that there is a symmetry operation ($\hat{S}$), which transforms the

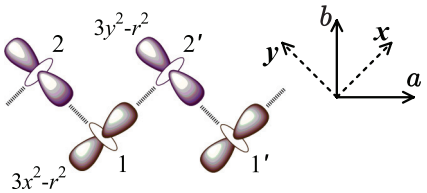

FIG. 3. (Color online) Geometry of the zigzag chain for the square lattice and the occupied e_g orbitals of the $3x^2 - r^2$ and $3y^2 - r^2$ types. Cubic and orthorhombic axes are denoted as $\boldsymbol{x}\,\boldsymbol{y}$ and $\boldsymbol{a}\boldsymbol{b}$, respectively.

zigzag chain to itself and which consists of the 180° rotation around the $\boldsymbol{a}$ axis ($\hat{C}_a^2$) with a consequent translation. For the $Pbnm$ structure (and with some appropriate choice of the origin), $\hat{S} = \{\hat{C}_a^2|\boldsymbol{a}/2 + \boldsymbol{b}/2\}$ (where the first part stands for the rotation, and the second part specifies the translation), while for the $P2_1nm$ structure, $\hat{S} = \{\hat{C}_a^2|\boldsymbol{a}/2 + \boldsymbol{c}/2\}$. It is important that both symmetry operations include the translation $\boldsymbol{a}/2$ and connect the sites 1 and 2. Then, it is convenient to work in the local basis, corresponding to the diagonal presentation of the e_g level splitting, such that $\hat{S}$ would transform the basis functions of the site 1 to those of the site 2, and vice versa. Our idea is that, although we have two different sites, with such choice of the basis functions, the Hamiltonian becomes periodic with the period $\boldsymbol{a}/2$ and the problem can be treated as if we would have only one site in the primitive cell. A similar idea was used for the analysis of the CE AFM phase in the half-doped manganites.[26] Rather generally, these basis functions can be chosen in the form

$$|1\rangle_1 = -\cos\beta|3z^2 - r^2\rangle_1 - \sin\beta|x^2 - y^2\rangle_1, \quad (8)$$

$$|2\rangle_1 = \sin\beta|3z^2 - r^2\rangle_1 - \cos\beta|x^2 - y^2\rangle_1 \quad (9)$$

at the site 1, and

$$|1\rangle_2 = -\cos\beta|3z^2 - r^2\rangle_2 + \sin\beta|x^2 - y^2\rangle_2, \quad (10)$$

$$|2\rangle_2 = \sin\beta|3z^2 - r^2\rangle_2 + \cos\beta|x^2 - y^2\rangle_2 \quad (11)$$

at the site 2, where $-\pi/2 < \beta \leqslant \pi/2$. $|\beta| = 60°$ corresponds to the ideal square lattice, subjected to the JT distortion, whose direction is controlled by anharmonic electron-lattice interactions.[16,27] Then, all deformations of the OO pattern are described by the single parameter β. Here, we continue to use the notations $|3z^2 - r^2\rangle$ and $|x^2 - y^2\rangle$ for the e_g orbitals, although it should be understood that they are valid only for the ideal square lattice. More generally, we have in mind some $|3z^2 - r^2\rangle$-like orbitals, which transform to each other as $\hat{S}|3z^2 - r^2\rangle_1 = |3z^2 - r^2\rangle_2$, and some $|x^2 - y^2\rangle$-like orbitals, which transform to each other as $\hat{S}|x^2 - y^2\rangle_1 = -|x^2 - y^2\rangle_2$. By substituting $\beta = -60°$ in Eqs. (8)–(11), one can find that $|1\rangle_1 = |3x^2 - r^2\rangle_1$, $|2\rangle_1 = |y^2 - z^2\rangle_1$, $|1\rangle_2 = |3y^2 - r^2\rangle_2$, and $|2\rangle_2 = |x^2 - z^2\rangle_1$. Similar analysis for $\beta = 60°$ yields $|1\rangle_1 = |3y^2 - r^2\rangle_1$, $|2\rangle_1 = |z^2 - x^2\rangle_1$, $|1\rangle_2 = |3x^2 - r^2\rangle_2$, and $|2\rangle_2 = |z^2 - y^2\rangle_2$. Then, although in realistic situations $|\beta|$ can deviate from 60°, we will say that $\beta < 0$ corresponds to the $3x^2 - r^2/3y^2 - r^2$ type of OO (referring to the type of the occupied orbitals at the sites 1 and 2), while $\beta > 0$ corresponds to the $3y^2 - r^2/3x^2 - r^2$ type of OO. It is important that, due to the symmetry operation $\hat{S}$, the OO is of the antiferro-type.

As for the transfer integrals between e_g orbitals, we again consider a more general case and write them in the following form:

$$\hat{t}_{12'} = \hat{t}_{2'1} = -\frac{t_0}{2}(\hat{\mathbb{I}} - |\sin\beta|\hat{\sigma}_x - \cos\beta\hat{\sigma}_z) \quad (12)$$

for the bond 1-2′, and

$$\hat{t}_{12} = \hat{t}_{21} = -\frac{t_0}{2}(\hat{\mathbb{I}} + |\sin\beta|\hat{\sigma}_x - \cos\beta\hat{\sigma}_z) \quad (13)$$

for the bond 1-2, in terms of the pseudospin Pauli matrices $\hat{\sigma}_x$, $\hat{\sigma}_y$, and $\hat{\sigma}_z$, and the 2×2 identity matrix $\hat{\mathbb{I}}$. The form of $\hat{t}_{ij}$ is suggested by the $dd\sigma$ transfer integrals in the ideal square lattice,[28] which again corresponds to $\beta = 60°$. Then, all deviations from the ideal square lattice are described by the single parameter β, similar to OO. Moreover, the form of Eqs. (12) and (13) is chosen so to satisfy the idempotency condition $(\hat{t}_{ij})^2 = t_0\hat{t}_{ij}$, which holds for the $dd\sigma$ type of transfer integrals,[28] and the time-reversal symmetry $\hat{t}_{ij}^* = \hat{t}_{ij}$.

Thus, in our model, the OO and the transfer integrals are described by the same parameter β. Generally speaking, these are different quantities, which should be described by two different sets of parameters. Nevertheless, in the analytically solvable model, one would always like to keep transparency and reduce the number of independent parameters to the minimum. Moreover, the use of the single parameter β is indeed very reasonable for our purposes. (i) At least for the ideal square lattice, the OO and the transfer integrals can be described by the same $|\beta| = 60°$. Thus, there is the reference point where our construction is exact. (ii) Small deviations from the ideal case are treated as an approximation and we have some freedom to decide the form of this approximation. In Sec. III B, we will show that typical deviations of $|\beta|$ from 60° are small and, therefore, our approximation is robust. Nevertheless, one important requirement is that the transfer integrals do not depend on the sign of β, while the OO does: the former are determined solely by the geometry of the zigzag chain, while the latter can be of two different types for the same chain.

After the transformation to the local basis, given by Eqs. (8)–(11), the transfer integrals become

$$\hat{\mathrm{t}}_{12'} = \hat{\mathrm{t}}_{21} = \frac{t_0}{2}(\cos\beta\hat{\mathbb{I}} + \sin 2\beta\hat{\sigma}_x - i|\sin\beta|\hat{\sigma}_y - \cos 2\beta\hat{\sigma}_z) \quad (14)$$

and $\hat{\mathrm{t}}_{2'1} = \hat{\mathrm{t}}_{12} = \hat{\mathrm{t}}_{21}^T$. Thus, unless $\beta = 0$ modulo $\pi/2$, $\hat{\mathrm{t}}_{ij}$ has both symmetric and antisymmetric parts, even despite the fact that the original $\hat{t}_{ij}$ was symmetric. This effect is caused by antiferro-OO and crucially important for understanding the origin of the FE activity. The transfer integrals are indeed periodic with the period $\boldsymbol{a}/2$ and, in the reciprocal space, the problem is reduced to the analysis of the 2×2 Hamiltonian

$$\hat{\mathcal{H}}(k) = \varepsilon(k) + \mathbf{d}(k) \cdot \hat{\boldsymbol{\sigma}},$$

where, in units of t_0, $\varepsilon(k) = \cos\beta\cos(ka/2)$, and components of the vector $\mathbf{d} \equiv (d_x, d_y, d_z)$ are given by $d_x = \sin 2\beta\cos(ka/2)$, $d_y = |\sin\beta|\sin(ka/2)$, and $d_z = -\cos 2\beta\cos(ka/2) - \Delta/2$. The parameter Δ in d_z is the intra-atomic energy splitting between e_g states, caused by lattice distortions and Coulomb interactions. Thus, the transformation to the local basis effectively "straightens" the zigzag chain and makes it equivalent to a linear chain, but with different transfer integrals operating in the positive and negative directions of $\boldsymbol{a}$. Because of the condition $\hat{\mathrm{t}}_{12} = \hat{\mathrm{t}}_{21}^T$, the transfer integrals are generally not centrosymmetric with respect to the Mn sites and, in the combination with finite Δ, the system will develop a finite electronic polarization. Nevertheless, in the limit $\Delta \to \infty$, the basis orbitals of the type "2" are projected out. Then, the transfer integrals between orbitals of the same type "1" are just scalars, and the condition $\hat{\mathrm{t}}_{12} = \hat{\mathrm{t}}_{21}^T$ becomes equivalent to $\mathrm{t}_{12} = \mathrm{t}_{21}$. Thus, in the limit $\Delta \to \infty$, the problem becomes

"centrosymmetric" and we use it as the reference point for the analysis of electronic polarization.

The eigenvalues of $\hat{\mathcal{H}}(k)$ are given by $E_{\pm}(k) = \varepsilon(k) \pm |\mathbf{d}(k)|$, and the eigenvector, corresponding to the lowest occupied band, satisfies the condition $[\mathbf{d}(k)\cdot\hat{\boldsymbol{\sigma}} + |\mathbf{d}(k)|]|-,k\rangle = 0$.[29] Then, $|-,k\rangle$ can be taken in the form

$$|-,k\rangle = \begin{pmatrix} C_1(k) \\ e^{i\gamma(k)}C_2(k) \end{pmatrix},$$

where

$$C_1(k) = \frac{1}{\sqrt{2}}\left(1 - \frac{d_z(k)}{|\mathbf{d}(k)|}\right)^{1/2},$$

$$C_2(k) = -\frac{1}{\sqrt{2}}\left(1 + \frac{d_z(k)}{|\mathbf{d}(k)|}\right)^{1/2},$$

and $\gamma(k) = \arctan(d_y/d_x)$.

At the half-filling (one e_g electron per each Mn site), the zigzag chain is an insulator, even for $\Delta = 0$.[30] Moreover, $|-,k\rangle$ is a periodic function of the reciprocal lattice vector of the "straightened" chain $G = 4\pi/a$. Therefore, the electronic polarization can be computed directly, using the formula of King-Smith and Vanderbilt.[12] Here, it is more convenient to work with the electric dipole moment rather than with the polarization density. Therefore, Eq. (3) was additionally multiplied by the primitive cell volume V. Nevertheless, unless it is specified otherwise, we will use the same notations for this quantity and continue to call it "the polarization". Then, we obtain the following expression for the FE polarization of the E phase (per two Mn sites in the zigzag chain):

$$P_E^{\mathrm{el}} = \frac{ea}{2\pi}\int_{-2\pi/a}^{2\pi/a} C_2^2(k)\frac{d\gamma(k)}{dk}dk,$$

which can be further transformed to

$$P_E^{\mathrm{el}} = \frac{ea^2}{4\pi}\int_0^{2\pi/a} \frac{|\sin\beta|\sin 2\beta}{|\mathbf{d}(k)|\,[|\mathbf{d}(k)| - d_z(k)]}dk. \qquad (15)$$

Thus, when the OO changes from $3x^2 - r^2/3y^2 - r^2$ ($\beta < 0$) to $3y^2 - r^2/3x^2 - r^2$ ($\beta > 0$), the polarization changes its sign. Then, one can find that

$$\lim_{\Delta\to 0^+} P_E^{\mathrm{el}} = \frac{|\sin\beta|}{\sin\beta}\frac{ea}{2}$$

and, therefore, $|P_E^{\mathrm{el}}| = ea/2$ (see Ref. 31). Then, since P_E^{el} is defined modulo ea,[12] the values of P_E^{el} and $-P_E^{\mathrm{el}}$ for $\Delta = 0$ are equivalent. Such a situation means that the system effectively possesses an inversion symmetry, but the inversion centers are located in the middles of the bonds.[32] Thus, by removing the JT distortion, we effectively create a new inversion center. This is indeed the case for the model considered above: since $\hat{t}_{ij} = \hat{t}_{ji}$, the transfer integrals are centrosymmetric with respect to the middles of the bonds. Nevertheless, we would like to emphasize that such behavior of P_E^{el} for $\Delta = 0$ is more general than simply the consequence of the inversion symmetry. In fact, the limit $|P_E^{\mathrm{el}}| = ea/2$ holds for the more general form of transfer integrals $\hat{t}_{ji} = \hat{t}_{ij}^T$, being the consequence of Hermiticity and the time-reversal symmetry of the DE Hamiltonian. The derivation is very straightforward and can be performed along the same line as above. Particularly, after removing the JT distortion, all considered compounds behave as "centrosymmetric" (in the sense that $|P_E^{\mathrm{el}}| = ea/2$), even despite the fact that the transfer integrals obey the orthorhombic $Pbnm$ and $P2_1nm$ symmetries with no inversion centers in the middles of the bonds (see Sec. III B). From this point of view, $\Delta = 0$ can be used as another reference point for P_E^{el}. For example, this choice was adopted in the work of Barone *et al.*[20]

In the limit $\Delta \to \infty$, we have

$$P_E^{\mathrm{el}}(\Delta \to \infty) \to \frac{ea|\sin\beta|\sin 2\beta}{\Delta^2}. \qquad (16)$$

Thus, P_E^{el} is proportional to both symmetric and antisymmetric components of $\hat{\mathbf{t}}_{ij}$, given by $\sin 2\beta$ and $|\sin\beta|$, respectively [see Eq. (14)]. This result has a transparent physical meaning and can be easily understood by starting from the expression

$$P_E^{\mathrm{el}} = -2e\int x w^2(x)dx, \qquad (17)$$

in terms of the Wannier functions,[12] where the prefactor 2 stands for the number of Mn sites in the primitive cell of the zigzag chain. Let us consider the limit $\Delta \to \infty$, where $|w_\infty\rangle = |1\rangle_1$ and is centered at the site 1 (see Fig. 3). Then, in the first order of $1/\Delta$, this Wannier function will have a finite tail, spreading to the neighboring sites 2 and 2′, which are located at $x = -a/2$ and $a/2$, respectively. In the first order of the perturbation theory, this tail is proportional to the transfer integrals t_{12}^{12} and $\mathrm{t}_{12'}^{12}$ from the occupied orbital $|1\rangle_1$ to the subspace of unoccupied orbitals $|2\rangle$ at the sites 2 and 2′ [see Eq. (14)]. Then, by assuming that all weights of $w^2(x)$ are accumulated at the lattice points (that is the meaning of the "lattice model"), one can write

$$w^2(x) = (1 - q_- - q_+)\delta(x) + q_-\delta(x + a/2) + q_+\delta(x - a/2),$$

where

$$q_{\pm} = \left(\frac{\sin 2\beta \mp |\sin\beta|}{2\Delta}\right)^2$$

are the weights of $w^2(x)$ at the sites 2 and 2′. By substituting $w^2(x)$ in Eq. (17), we again arrive at Eq. (16). Thus, in terms of these arguments, the polarization is finite because $q_+ \neq q_-$ and the Wannier centers are shifted from the centrosymmetric atomic positions.[14,20]

A very similar model was considered recently by Barone *et al.*[20] The advantage of our approach is that we were able to reduce the problem to the 2×2 Hamiltonian in the reciprocal space and to solve it analytically. Thus, we could gain much insight in the origin of electronic polarization. The results of Barone *et al.* are seemingly different from ours: $P_E^{\mathrm{el}} = 0$ for $\Delta = 0$ and approaches $\pm ea/2$ for $\Delta \to \infty$. Nevertheless, this difference is related to the different choice of the reference point in for P_E^{el}: $\Delta \to \infty$ in our work and $\Delta = 0$ in the work of Barone *et al.*[33] In terms of considered model, both choices are legitimate, as they restore the inversion symmetry of the DE Hamiltonian. Nevertheless, in the $Pbnm$ structure, the inversion centers coincide with the positions of the Mn sites, which correspond to the choice $\Delta \to \infty$ in the model analysis. Therefore, the reference point $\Delta \to \infty$ is more suitable for the analysis of first-principles calculations because the latter are always based on the actual symmetry of the system.

TABLE I. Parameters of the e_g model for the isolated zigzag chain, derived for $HoMnO_3$ (HMO) and different structures of $YMnO_3$ (YMO): the experimental $Pbnm$ and $P2_1nm$ structures, reported in Ref. 21, and three theoretical $P2_1nm$ structures, optimized in LSDA and LDA $+U$ with $U=2.2$ and 6.0 eV (results of Ref. 10). In this table, t_0 is the effective two-center integral, Δ is the intra-atomic splitting between e_g states, and β specifies the form of the transfer integrals in the Mn-Mn bonds. The values, obtained by using bare LDA parameters are denoted as LDA, and the ones after adding the Hartree-Fock potential are denoted as "$+U$."

	t_0 (meV)		Δ (eV)		β (degrees)	
	LDA	$+U$	LDA	$+U$	LDA	$+U$
HMO ($Pbnm$, Expt.)	341	353	1.52	2.15	−54.0	−55.3
YMO ($Pbnm$, Expt.)	335	348	1.53	2.18	−54.2	−55.8
YMO ($P2_1nm$, Expt.)	334	346	1.54	2.15	−54.1	−55.7
YMO ($P2_1nm$, LSDA)	405	412	0.92	1.95	57.6	59.1
YMO ($P2_1nm$, $U=2.2$ eV)	361	370	1.37	2.41	55.1	57.3
YMO ($P2_1nm$, $U=6.0$ eV)	348	359	1.30	2.04	54.4	56.1

B. Parameters of the e_g model and values of electronic polarization for $YMnO_3$ and $HoMnO_3$

In this section, we evaluate parameters of the e_g model for realistic compounds, such as $YMnO_3$ and $HoMnO_3$. For these purposes, we do the following:

(i) start with the realistic low-energy model, derived for the Mn $3d$ bands on the basis of first-principles electronic-structure calculations (results of Refs. 10 and 25);

(ii) pick up parameters for a single zigzag chain, propagating along the $\boldsymbol{a}$ axis;

(iii) find eigenvalues and eigenfunctions for the isolated chain;

(iv) construct the Wannier functions for the upper lying e_g bands; for these purposes, we use the projector-operator technique and trial orbitals, obtained from the diagonalization of the site-diagonal part of the density matrix;[24]

(v) find parameters of the e_g model in the Wannier basis;

(vi) transform obtained parameters to the CF representation, diagonalizing the site-diagonal part of the e_g model;

(vii) derive parameters t_0 and β from the fitting of transfer integrals in the form of Eq. (14), and the energy splitting Δ from the site-diagonal part.

For $YMnO_3$, we have considered several crystal structures, which were previously discussed in Ref. 10: (i) the experimental $Pbnm$ and $P2_1nm$ structures, reported in Ref. 21; (ii) three theoretical $P2_1nm$ structures, optimized in the local-spin-density approximation (LSDA) and LDA $+ U$ with $U=2.2$ and 6.0 eV by assuming the collinear E-type AFM alignment. The results of this optimization can be found in Ref. 10.

For $HoMnO_3$, we use the experimental $Pbnm$ structure, reported in Ref. 34. Parameters of the e_g model, obtained from the fitting, are summarized in Table I.[35]

In Fig. 4, we plot results of analytically solvable model (see Sec. III A) and the actual numerical values of $P_E^{\rm el}$, obtained for the e_g band without fitting (for the abscissa coordinates, we use the values from Table I). One can clearly see that all these numerical values fall on the analytical dependence, derived for the e_g model. The main parameter, which controls the value of $P_E^{\rm el}$, is the ratio Δ/t_0. The β dependence is less important. Moreover, the physically relevant situation, realized in orthorhombic manganites, always corresponds to the limit of large Δ. This property holds even in bare LDA and is additionally strengthened after including the on-site Coulomb repulsion. This is a very important finding, which will allow us to further rationalize the behavior of the FE polarization in Sec. III C.

The polarization has a different sign for the experimental and theoretical structures, which indicates different types of the OO in the zigzag chain. In the $Pbnm$ phase, all zigzag chains are equivalent, and in Fig. 4 we simply picked up the one with the same OO as in the experimental $P2_1nm$ phase. However, in the $P2_1nm$ phase, the type of the zigzag chain is uniquely defined (the one with larger Mn-Mn distances, which are favorable for FM interactions). Therefore, the sign difference between experimental and theoretical values of

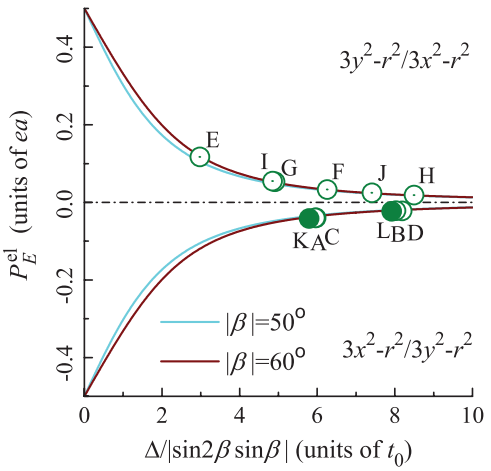

FIG. 4. (Color online) Electric dipole moment for isolated zigzag chain as the function of intra-atomic energy splitting between e_g states. Upper part corresponds to the $3y^2-r^2/3x^2-r^2$ type of the orbital ordering ($\beta>0$) and lower part corresponds to the $3x^2-r^2/3y^2-r^2$ type of the orbital ordering ($\beta<0$). The values obtained for $YMnO_3$ are shown by open symbols. The points A, C, E, G, and I denote the bare LDA values, obtained for the experimental $P2_1nm$ and $Pbnm$ structures, and three theoretical structures, obtained in LSDA and LDA $+ U$ with $U=2.2$ and 6.0 eV, respectively. Similar values, obtained after adding the HF potentials, are denoted as B, D, G, H, and J, respectively. The values obtained for the experimental $Pbnm$ structure of $HoMnO_3$ are shown by filled symbols: the point K denotes the bare LDA value and the point L takes into account the effect of the HF potential.

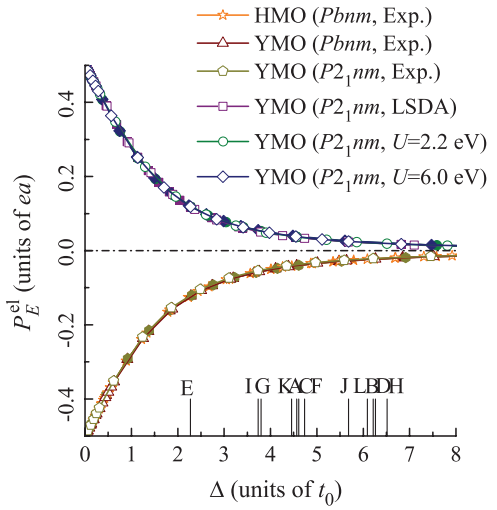

FIG. 5. (Color online) Electric dipole moment versus Δ/t_0, as obtained using various sets of parameters for the e_g model. Results of bare LDA and after adding the Hartree-Fock potential are shown by filled and open symbols, respectively. The positions of Δ/t_0 for different systems are shown by capital letters. The points A, C, E, G, and I stand for the bare LDA values of Δ/t_0, corresponding to the experimental $P2_1nm$ and $Pbnm$ structures, and three theoretical structures, obtained in LSDA and LDA + U with $U=$ 2.2 and 6.0 eV, respectively. Similar points, obtained after adding the Hartree-Fock potential, are denoted as B, D, G, H, and J, respectively. The points K and L correspond to the $Pbnm$ structure of $HoMnO_3$, obtained in the bare LDA and after adding the HF potential, respectively.

P_E^{el} in the $P2_1nm$ phase indicates a serious problem, which may exist in first-principles calculations. The problem will be discussed in details in Sec. III D.

Then, all values of $|\beta|$ are close to $|\beta_{max}| = \arctan\sqrt{2} \approx 54.7^\circ$, corresponding to the maximum of $|P_E^{el}|$ [see Eq. (16)]. Therefore, the effect of β on P_E^{el} is small, and $P_E^{el}(\beta)$ will deviate from $P_E^{el}(\beta_{max})$ only of the second order of $(\beta - \beta_{max})$. This can be clearly seen in Fig. 5, where we plot P_E^{el} versus Δ/t_0, using different sets of parameters for the e_g model and varying Δ: all lines, corresponding to different crystal structures and different levels of approximation for the on-site interactions (with and without the HF potential), are practically undistinguishable. Moreover, in these calculations we use actual transfer integrals, without fitting. This means that, in reality, P_E^{el} is controlled by only two sets of parameters: (i) the ratio Δ/t_0, and (ii) the lattice parameters a, b, and c, which determine the value of the scaling factor a/V in the polarization density. The β dependence of P_E^{el} is relatively unimportant. Note also that for $\Delta = 0$ we identically have $|P_E^{el}| = ea/2$, even for realistic transfer integrals obeying the $Pbnm$ and $P2_1nm$ symmetry, as the consequence of the time-reversal symmetry of the DE Hamiltonian (see discussions in Sec. III A).

From the physical point of view, the β dependence of transfer integrals is related to the buckling of the Mn-O-Mn bonds. Then, the above result suggests that P_E^{el} does not explicitly depend on the Mn-O-Mn angles: the latter can contribute to P_E^{el}, but only via other model parameters (such as t_0), which also depend on these angles. This finding is consistent with the conclusion of Ref. 14, based on the first-principles calculations.

Finally, we briefly explain the correspondence between the values of the electric dipole moment in Fig. 4 and the polarization density. Let us consider the experimental $Pbnm$ structure of $YMnO_3$. Then, the value $-0.022ea$, after including the HF potential, corresponds to the polarization density of -1.65 μC/cm^2. It should be remembered that it is the contribution of the e_g band alone. In order to obtain the total polarization of the five-orbital model, it should be combined with the contribution of the t_{2g} band. This yields the total polarization of -0.84 μC/cm^2, which agrees with the value for the E-type AFM state ($\phi = 180^\circ$ in Fig. 2). Thus, the contributions of the t_{2g} and e_g bands have opposite sign and partially cancel each other, in agreement with the first-principles calculations.[14] In the rest of this work, we will deal with the total polarization density, including the effect of both t_{2g} and e_g bands.

C. Electronic polarization in the five-orbital model: Simple analytical expression

Now, we will generalize results of two previous sections and derive an approximate, but very transparent, expression for the electronic polarization in orthorhombic manganites with a general twofold periodic magnetic texture. Our starting point is that the behavior of electronic polarization in realistic manganites always corresponds to the limit of large Δ. Thus, the central quantity, which we should evaluate in the second order of $1/\Delta$, is the weight $w^2_{i\to j}$, transferred from the Wannier orbital at the site i to the neighboring site j. Moreover, since electronic polarization is equal to zero for the fully occupied band, it is more convenient to start with the unoccupied e_g orbitals and consider the transfer integrals to the subspace of three t_{2g} and one e_g occupied orbitals at each of the neighboring sites. This procedure should give us $-\mathbf{P}^{el}$.

The transfer integrals obey certain symmetry rules and, in the DE model, are additionally modulated by ξ_{ij}. More specifically, we consider a planar magnetic texture, shown in Fig. 6. The periodicity of this texture along the orthorhombic axes is a and $2b$, respectively. The directions of spins are specified by three azimuthal angles: ϕ_2, ϕ_3, and ϕ_4 (while $\phi_1 = 0$ is treated as the reference point). Moreover, we assume that the DE Hamiltonian remains invariant under

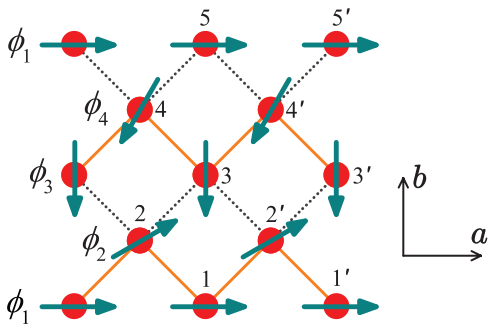

FIG. 6. (Color online) General twofold periodic magnetic texture in the ab plane of orthorhombic manganites, which remains invariant under the symmetry operation $\hat{S} = \{\hat{C}_a^2|\boldsymbol{a}/2 + \boldsymbol{b}/2\}$. Solid and dotted lines denote two types of magnetically inequivalent bonds.

the symmetry operation $\hat{S} = \{\hat{C}_a^2|\boldsymbol{a}/2+\boldsymbol{b}/2\}$, which transforms the bond 1-2 to 4′-3, the bond 3-2 to 4′-5, etc. In the DE model, it imposes additional conditions: $\cos\frac{\phi_2}{2} = \cos\frac{\phi_3-\phi_4}{2}$ and $\cos\frac{\phi_4}{2} = \cos\frac{\phi_3-\phi_2}{2}$, which are simultaneously satisfied when $\phi_3 = \phi_2 + \phi_4$ (modulo 4π). Thus, the magnetic texture is specified by only two independent parameters ϕ_2 and ϕ_4, similar to the magnetic ground state, obtained in the mean-field HF calculations with the SO coupling.[9,10]

Then, we consider some central site (say, site 3 in Fig. 6) and evaluate its contribution to the vector of electronic polarization, which is caused by the Wannier weight transfer to the neighboring sites 4′, 4, 2, and 2′, located at $(\boldsymbol{a}+\boldsymbol{b})/2$, $-(\boldsymbol{a}-\boldsymbol{b})/2$, $-(\boldsymbol{a}+\boldsymbol{b})/2$, and $-(\boldsymbol{a}-\boldsymbol{b})/2$, respectively. In the second order of $1/\Delta$ (and apart from the proportionality coefficient, which will be specified later), this contribution is given by

$$\mathbf{P}_3^{\rm el} \sim \frac{e}{2}\cos^2\frac{\phi_2}{2}\left[(\boldsymbol{a}+\boldsymbol{b})w^2_{3\to 4'} - (\boldsymbol{a}-\boldsymbol{b})w^2_{3\to 4}\right] + \frac{e}{2}\cos^2\frac{\phi_4}{2}\left[(\boldsymbol{a}-\boldsymbol{b})w^2_{3\to 2'} - (\boldsymbol{a}+\boldsymbol{b})w^2_{3\to 2}\right], \quad (18)$$

where $w^2_{i\to j}$ is proportional to the sum of squares of the transfer integrals from the unoccupied orbital 5 at the site i to the occupied orbitals 1–4 at the site j: $w^2_{i\to j} = [(\mathrm{t}^{51}_{ij})^2 + (\mathrm{t}^{52}_{ij})^2 + (\mathrm{t}^{53}_{ij})^2 + (\mathrm{t}^{54}_{ij})^2]/\Delta^2$. These transfer integrals should be calculated in the CF representation, which diagonalizes the site-diagonal part of the DE Hamiltonian. The parameter Δ is understood as the energy difference between unoccupied orbital 5 and the center of gravity of occupied orbitals 1–4 (see Fig. 7). Thus, we neglect the splitting between occupied orbitals, which is smaller than Δ. Then, in the $Pbnm$ structure, each Mn site is located in the inversion center. Therefore, $w^2_{i\to j}$ in the bonds 3-4′ and 3-2 (as well as 3-2′ and 3-4) are

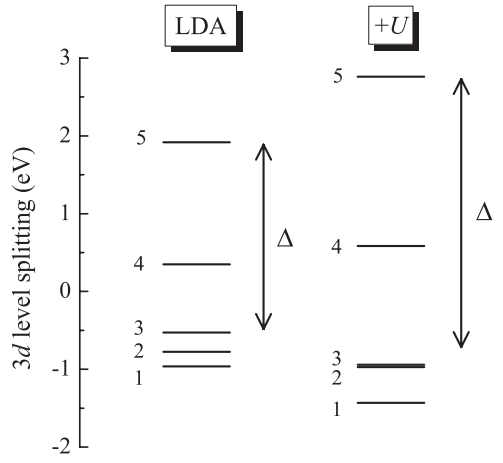

FIG. 7. Splitting of 3d levels for the experimental $Pbnm$ phase of $YMnO_3$. The values, obtained using bare LDA parameters of the low-energy model, are denoted as LDA, and those obtained after adding the Hartree-Fock potential are denoted as $+U$. Δ is the energy splitting between the unoccupied orbital 5 and the center of gravity of occupied orbitals 1–4.

equivalent, and Eq. (18) can be further transformed to

$$\mathbf{P}_3^{\rm el} \sim \frac{e}{4}(\cos\phi_2 - \cos\phi_4)\left[(\boldsymbol{a}+\boldsymbol{b})w^2_{3\to 4'} - (\boldsymbol{a}-\boldsymbol{b})w^2_{3\to 4}\right]. \quad (19)$$

Similar analysis can be performed for another Mn site in the primitive cell (say, site 4′ in Fig. 6). Moreover, since the sites 3 and 4′ are connected by $\hat{S} = \{\hat{C}_a^2|\boldsymbol{a}/2+\boldsymbol{b}/2\}$, $\mathbf{P}_{4'}^{\rm el}$ can be obtained from Eq. (19) as

$$\mathbf{P}_{4'}^{\rm el} \sim \frac{e}{4}(\cos\phi_2 - \cos\phi_4)\left[(\boldsymbol{a}-\boldsymbol{b})w^2_{3\to 4'} - (\boldsymbol{a}+\boldsymbol{b})w^2_{3\to 4}\right].$$

Then, the total polarization $\mathbf{P}^{\rm el} = 2(\mathbf{P}_3^{\rm el} + \mathbf{P}_{4'}^{\rm el})$ is

$$\mathbf{P}^{\rm el} = \frac{e}{V}(\cos\phi_2 - \cos\phi_4)\left[w^2_{3\to 4'} - w^2_{3\to 4}\right]\boldsymbol{a},$$

where V is the primitive cell volume, containing four Mn sites (that leads to the additional prefactor 2). Finally, the sites 3 and 4 can be transformed by $\hat{S} = \{\hat{C}_a^2|\boldsymbol{a}/2+\boldsymbol{b}/2\}$ to the sites 4′ and 3, respectively. Then, $\mathbf{P}^{\rm el}$ can be expressed through the transfer integrals in only one nearest-neighbor (NN) bond 3-4′ (or in any other equivalent to it bond):

$$\mathbf{P}^{\rm el} = \tfrac{1}{2}(\cos\phi_2 - \cos\phi_4)\mathbf{P}_E^{\rm el}, \quad (20)$$

where

$$\mathbf{P}_E^{\rm el} = \frac{2e}{V}\left[w^2_{3\to 4'} - w^2_{4'\to 3}\right]\boldsymbol{a} \quad (21)$$

is the electronic polarization of the E phase. For an arbitrary direction of spin at the site 1, $(\cos\phi_2 - \cos\phi_4)$ in Eq. (20) should be replaced by $\mathbf{e}_1\cdot(\mathbf{e}_2 - \mathbf{e}_4)$. Equations (20) and (21) allow us to rationalize many aspects of multiferroic activity in orthorhombic manganites with the twofold periodic magnetic texture, namely, (i) $\mathbf{P}^{\rm el}$ is parallel to the $\boldsymbol{a}$ axis. (ii) When $\phi_4 = \phi_2 + \pi$, $\mathbf{P}^{\rm el}$ is proportional to $\cos\phi_2$. It explains the functional dependence of $\mathbf{P}^{\rm el}(\phi)$ in Fig. 2(b) and in the first-principles calculations for the same magnetic geometry (Ref. 5). (iii) $\mathbf{P}^{\rm el}$ vanishes in the homogeneous spin-spiral state ($\phi_2 = \pi/2$ and $\phi_4 = 3\pi/2$). This is a natural result from the viewpoint of the DE physics: in the spin-spiral phase, all ξ_{ij} are the same. Therefore, all bonds remain equivalent and the inversion symmetry is not broken. (iv) Since $\hat{\mathrm{t}}_{ji} = \hat{\mathrm{t}}^T_{ij}$, $\mathbf{P}_E^{\rm el}$ can be also presented in the form

$$\mathbf{P}_E^{\rm el} = \frac{2e}{V}\frac{(\vec{v}_+,\vec{v}_-)}{\Delta^2}\boldsymbol{a}, \quad (22)$$

where $(\vec{v}_+,\vec{v}_-)$ is the scalar product of the four-dimensional vectors $\vec{v}_\pm \equiv (v^1_\pm, v^2_\pm, v^3_\pm, v^4_\pm)$, constructed from symmetric (+) and antisymmetric (−) parts of the transfer integrals $v^m_\pm = \mathrm{t}^{5m}_{ij} \pm \mathrm{t}^{m5}_{ij}$. Thus, in order to have finite $\mathbf{P}^{\rm el}$, the matrix of transfer integrals should have both symmetric and antisymmetric components in the CF representation. In the $\boldsymbol{ab}$ plane, the main contribution to this asymmetry comes from the antiferro-OO (see Sec. III A).

Let us evaluate $\mathbf{P}_E^{\rm el} \equiv (P_E^{\rm el},0,0)$ using Eq. (22) for the experimental $Pbnm$ phase of $YMnO_3$. In this case, the unit-cell volume V is 224.13 Å^3 and the orthorhombic lattice parameter a is 5.245 Å.[21] Then, for the bare LDA case, we have $\Delta = 2.40$ eV (see Fig. 7), $\vec{v}_+ = (-125, 18, 15, 336)$ meV, and $\vec{v}_- = (99, -49, -25, -314)$ meV (all parameters can be found in the Supplemental Material of Ref. 10). By substituting all

these values in Eq. (22), we obtain $P_E^{\rm el} = -1.55\ \mu{\rm C/cm}^2$, which agrees very well with the value of $-1.53\ \mu{\rm C/cm}^2$, obtained directly from the Berry-phase formula [Eq. (3)], without additional approximations (apart from the DE limit). After adding the HF potential, we have $\Delta = 3.45$ eV, $\vec{v}_+ = (6,-117,26,335)$ meV, and $\vec{v}_- = (10,91,-24,-319)$ meV. Then, Eq. (22) yields $P_E^{\rm el} = -0.74\ \mu{\rm C/cm}^2$, which is again consistent with the value of $-0.85\ \mu{\rm C/cm}^2$, obtained from the Berry phase formula. Moreover, the scalar product $(\vec{v}_+,\vec{v}_-)$ practically does not depend on whether it is calculated with or without the HF potential: -0.118 and -0.119 eV^2, respectively. Nevertheless, this is to be expected because the form of the CF orbitals in manganites is mainly controlled by the JT distortion: the latter is large and thus "decides" which orbitals will be occupied and which will not. On the other hand, the effect of on-site Coulomb interactions, being inversely proportional to U,[16] is considerably weaker. Thus, although the Coulomb interactions contribute to the splitting Δ (see Fig. 7), they practically do not change the subspace of occupied states and therefore $(\vec{v}_+,\vec{v}_-)$.

Furthermore, Δ can be presented in the form $\Delta = \Delta_{\rm JT} + \Delta_U$, where $\Delta_{\rm JT}$ and Δ_U take into account the effects of the bare JT distortion and the on-site Coulomb interactions, respectively. In the example considered above, $\Delta_{\rm JT}$ is the LDA level splitting and Δ_U is the additional splitting, caused by the HF potential. Then, if $P_E^{\rm el}(0)$ is the FE polarization in LDA, the effect of on-site Coulomb interactions on $P_E^{\rm el}$ can be evaluated using the scaling relation

$$P_E^{\rm el}(\Delta_U) = P_E^{\rm el}(0)\big/(1+\Delta_U/\Delta_{\rm JT})^2,$$

which was indeed observed in many LDA + U calculations, treating the on-site Coulomb repulsion U as an adjustable parameter.[5,21]

Finally, it is instructive to evaluate $\mathbf{P}^{\rm el} \equiv (P^{\rm el},0,0)$ for the noncollinear magnetic ground state of $YMnO_3$ using Eq. (20). This magnetic ground state was obtained in Ref. 10 by solving mean-field HF equations with the SO interaction. For the $Pbnm$ phase of $YMnO_3$, it yields $\phi_2 = 60^\circ$ and $\phi_4 = 240^\circ$. Then, using $P_E^{\rm el} = -0.85\ \mu{\rm C/cm}^2$, obtained in the DE limit (see Fig. 2), $P^{\rm el}$ can be estimated as $-0.43\ \mu{\rm C/cm}^2$, which is consistent reasonably well with $P^{\rm el} = -0.55\ \mu{\rm C/cm}^2$, obtained for the noncollinear magnetic ground state of $YMnO_3$ without additional approximations.[10] In fact, the main discrepancy is caused by the DE limit for $P_E^{\rm el}$. For example, if one uses $P_E^{\rm el} = -1.04\ \mu{\rm C/cm}^2$, obtained without the DE approximation,[10] and the angular dependence, given by Eq. (20), $P^{\rm el}$ can be estimated as $-0.50\ \mu{\rm C/cm}^2$, which is much closer to $P^{\rm el} = -0.55\ \mu{\rm C/cm}^2$.

D. Relative directions of electronic and ionic polarizations, and problems of structural optimization in LDA + U

So far, we considered only electronic polarization, which was induced by the OO in the FM chains. In this section, we will discuss how this electronic part is connected with the ionic polarization in the noncentrosymmetric $P2_1nm$ structure. Moreover, we will elucidate the microscopic origin of the so-called "order of magnitude difference," which typically exists between experimental and theoretical values of the FE polarization, reported for twofold periodic manganites. The problem is formulated as follows. The first-principles calculations allow us to perform the structural optimization and to find atomic displacements, caused by the exchange-striction effects in the E-type AFM phase. If one does so for orthorhombic manganites and subsequently calculates the FE polarization, the latter will be of the order of several $\mu{\rm C/cm}^2$.[5] The conclusion is rather generic and was obtained for several popular types of the exchange-correlation functionals, such as LSDA (Ref. 10), generalized gradient approximation (GGA, Refs. 5 and 14), and LDA(GGA) + U (Refs. 5 and 10). The experimental polarization is typically smaller than $0.5\ \mu{\rm C/cm}^2$.[2] On the other hand, if one takes the experimental $P2_1nm$ structure and calculates the FE polarization, it will be at least of the same order of magnitude as the experimental one.[10,21] Moreover, in the experimental $P2_1nm$ structure, there is a large cancellation between electronic and ionic contributions to the FE polarization, while in the theoretically optimized structure, these two contributions have the same sign and the cancellation does not occur.[10]

In this section, we will further clarify the situation. In orthorhombic manganites, there are three types of atomic displacements, which control the FE polarization:

(i) The JT distortion, which gives rise to the OO.

(ii) The exchange striction, which specifies the type of the ordering in the FM zigzag chain and, therefore, the sign of electronic polarization. In the centrosymmetric $Pbnm$ structure, the FM chains with the $3x^2-r^2/3y^2-r^2$ and $3y^2-r^2/3x^2-r^2$ types of the OO are equivalent as they form two degenerate magnetic states. This degeneracy is lifted in the $P2_1nm$ phase by the exchange-striction effects, which pick up only one type of the FM zigzag chains (with larger Mn-Mn distances). As soon as the FM chains are selected, the type of the OO is also fixed, so as the sign of the electronic polarization.

(iii) The FE displacements of oxygen atoms, which occur in response to the magnetic inversion symmetry breaking and control the sign of the ionic polarization.

The goal of this section is to understand how these three types of the lattice distortions correlate with each other in the experimental and theoretically optimized $P2_1nm$ structures of $YMnO_3$.

Let us consider the ionic polarization and concentrate on the behavior of the oxygen sites, which are located in the $\boldsymbol{ab}$ plane and give the largest contribution to $\mathbf{P}_E^{\rm ion}$.[10] The contributions of other atomic sites do not alter our conclusion. Then, $\mathbf{P}_E^{\rm ion}$ can be presented in the following form:

$$\mathbf{P}_E^{\rm ion} = \frac{1}{2V}\sum_i Z_i \Delta\boldsymbol{\tau}_i, \tag{23}$$

where it is understood that around each Mn site in the primitive cell, the summation runs over four oxygen sites, located in the nearest neighborhood of Mn. Since each oxygen is shared by two Mn atoms, we added the prefactor 1/2 in Eq. (23). There are many possibilities for choosing the centrosymmetric reference point for $\mathbf{P}_E^{\rm ion}$. For our purposes, it is convenient to take $\Delta\boldsymbol{\tau}_i = \boldsymbol{\tau}_{\rm O} - \boldsymbol{\tau}_{\rm Mn}$ (in other words, we assume that in the centrosymmetric structure, all oxygen sites "fall" on the central Mn site). This can be done because Mn sites do not contribute to the ionic polarization parallel to the $\boldsymbol{a}$ axis.[10]

The reason is that, apart from a constant shift, the projections of Mn sites onto the $\boldsymbol{a}$ axis are either 0 or $a/2$ (modulo the lattice translation a) and, therefore, can be transformed to each other by the reflection $\boldsymbol{a} \to -\boldsymbol{a}$. The Mn sites do contribute to the ionic polarization in the $\boldsymbol{bc}$ plane. However, all these contributions have antiferroelectric character and cancel out after summation over the primitive cell. Thus, around each Mn site, the evaluation of $\mathbf{P}_E^{\rm ion}$ is reduced to the summation of coordinates of nearest oxygen sites. Such a construction is very convenient because in the centrosymmetric $Pbnm$ structure, each Mn site is located in the inversion center. Therefore, the sum of $\Delta\boldsymbol{\tau}_i$ over all neighboring Mn-O bonds will be equal to zero. In the $P2_1nm$ structure, however, such a construction will give us a finite vector, which can serve as a measure of noncentrosymmetric atomic displacements around each Mn site. For our purposes, only the $\boldsymbol{a}$ components of these vectors are important, while the $\boldsymbol{b}$ and $\boldsymbol{c}$ components are antiferroelectric and will cancel each other. Using this construction and $Z_{\rm O} = -2e$, the contribution of the planar oxygen sites to $P_E^{\rm ion}$ in the experimental $P2_1nm$ structure can be estimated as 0.73 μC/cm^2, which is totally consistent with the previous finding.[10]

The distributions of such vectors, obtained for the experimental and theoretical structures of $YMnO_3$, are shown in Figs. 8(a) and 8(c), respectively. As for the theoretically optimized structure, we use results of LDA + U calculations with $U = 2.2$ eV (see Ref. 10, very similar results were obtained in LSDA and LDA + U with $U = 6.0$ eV). As is seen in Fig. 8, the FE displacements have the same direction in the experimental and theoretically optimized structures. This direction corresponds to the positive value of $P_E^{\rm ion}$.

Corresponding OO, realized in the FM chains, is shown in Figs. 8(b) and 8(d) for the experimental and theoretical structures, respectively. For the experimental $P2_1nm$ structure, the OO is of the $3x^2 - r^2/3y^2 - r^2$ type. Therefore, the electronic polarization is negative, and there is a partial cancellation of the electronic and ionic terms, which explains the relatively small value of the experimental polarization.[10] However, in the theoretically optimized structure, the OO is different: $3y^2 - r^2/3x^2 - r^2$ instead of $3x^2 - r^2/3y^2 - r^2$. Therefore, the electronic polarization is positive, and the cancellation does not occur.

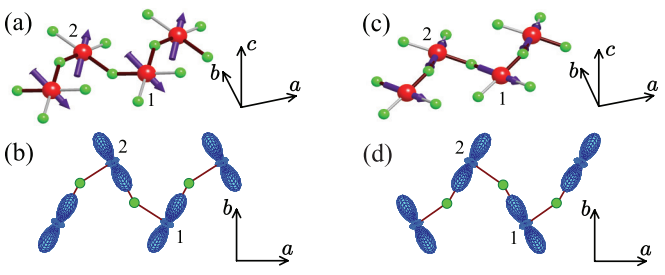

FIG. 8. (Color online) Directions of ionic contributions to the polarization, caused by ferroelectric displacements of oxygen atoms around each Mn site in the $\boldsymbol{ab}$ plane of noncentrosymmetric $P2_1nm$ phase of $YMnO_3$ [(a) and (c)], and the orbital ordering, realized in the ferromagnetic zigzag chain [(b) and (d)], as obtained for the experimental [(a) and (b)] and theoretically optimized structure [(c) and (d)].

Thus, the directions of FE displacements, obtained in LSDA and LDA + U, are inconsistent with the type of the OO, realized in the FM zigzag chains. This seems to be a serious problem of first-principles calculations and at the present stage there is not a clear clue as to how it should be solved. On the computational side, much attention is paid to the screened hybrid functionals (see, e.g., Ref. 36). Therefore, it would be interesting to see how these functionals will work for the structural optimization in improper ferroelectrics, where the inversion symmetry is broken by magnetic degrees of freedom. The first applications for $HoMnO_3$ seem to show that the problem persists and the total polarization is overestimated.[37] On the other hand, the directions of FE displacements can be controlled by the relativistic SO interaction, which is typically ignored in the process of structural optimization. This point of view was proposed, for example, in Ref. 38.

E. Switching electric polarization by changing the magnetic texture

What is interesting about multiferroics is that the value and direction of the FE polarization depend on the magnetic texture and, by manipulating with this texture, one can change the vector of polarization. In this section, we will discuss how such behavior can be realized in twofold periodic manganites. Again, let us consider the centrosymmetric $Pbnm$ structure and assume that the inversion symmetry is broken exclusively by the magnetic order. In such a case, most of the attention is paid to the E-type AFM phase (Fig. 2), which breaks the inversion symmetry but preserves the glide rotation $\{\hat{C}_a^2|\boldsymbol{a}/2 + \boldsymbol{b}/2\}$. Therefore, the FE polarization will be parallel to the $\boldsymbol{a}$ axis.

Now, the question is whether there are other textures, which would break the inversion symmetry. Let us consider the example shown in Fig. 9(a). In the plane $z = 0$, this texture is identical to the E phase, and can be transformed to itself by applying $\{\hat{C}_a^2|\boldsymbol{a}/2 + \boldsymbol{b}/2\}$ around even magnetic sites 2 and 4. Alternatively, one can apply $\{\hat{C}_a^2|-\boldsymbol{a}/2 - \boldsymbol{b}/2\}$ around odd magnetic sites 1 and 3. In the E phase, the same symmetry operations can be applied in the planes $z = \pm c/2$ and also will transform the plane $z = c/2$ to the equivalent to it plane $z = -c/2$. The magnetic texture in Fig. 9(a) is obtained by the additional inversion around odd magnetic sites in the plane $z = c/2$, which interchanges the symmetry operations $\{\hat{C}_a^2|\boldsymbol{a}/2 + \boldsymbol{b}/2\}$ and $\{\hat{C}_a^2|-\boldsymbol{a}/2 - \boldsymbol{b}/2\}$. Thus, the plane $z = c/2$ can be transformed to itself by $\{\hat{C}_a^2|\boldsymbol{a}/2 + \boldsymbol{b}/2\}$ around odd sites and by $\{\hat{C}_a^2|-\boldsymbol{a}/2 - \boldsymbol{b}/2\}$ around even sites. Therefore, the symmetry operations $\{\hat{C}_a^2|\boldsymbol{a}/2 + \boldsymbol{b}/2\}$ and $\{\hat{C}_a^2|-\boldsymbol{a}/2 - \boldsymbol{b}/2\}$, although preserved locally in each of the planes, are broken globally because they can not simultaneously transform the planes $z = 0$ and $\pm c/2$ to themselves. Instead, the magnetic texture in Fig. 9(a) is invariant under the glade rotation $\{\hat{C}_c^2|\boldsymbol{c}/2\}$ around even sites, which also belongs to the space group $Pbnm$. Therefore, the FE polarization will be parallel to the $\boldsymbol{c}$ axis.

The behavior of $\mathbf{P} \parallel \boldsymbol{c}$, obtained in the DE model for $YMnO_3$, is explained in Fig. 9(b). $\mathbf{P} \parallel \boldsymbol{c}$ appears to be about two orders of magnitude smaller than $\mathbf{P} \parallel \boldsymbol{a}$ in the E phase (see Fig. 2). Nevertheless, this result is very natural and can be

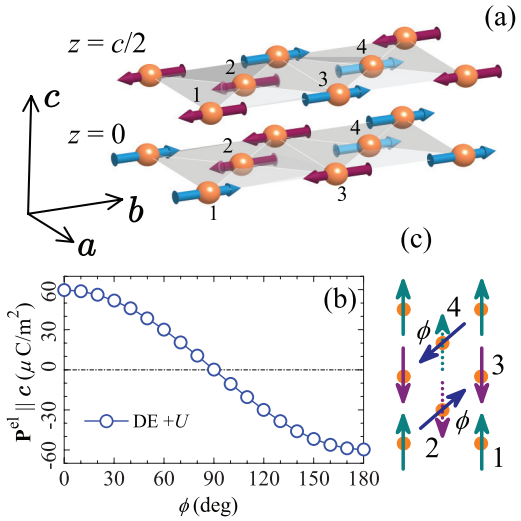

FIG. 9. (Color online) (a) Antiferromagnetic texture yielding finite ferroelectric polarization along the $\boldsymbol{c}$ axis. (b) Behavior of electronic polarization in $YMnO_3$ upon rotation of magnetic moments, as obtained in the double-exchange model with the Hartree-Fock potential $\hat{\mathcal{V}}_i^{\uparrow}$ (DE + U). In the rotated texture, the directions of spins at the sites 1 and 3 were fixed, while the spins at the sites 2 and 4 were rotated by the angle ϕ, as explained in panel (c). The interlayer coupling was kept AFM for the sites 1 and 3 and FM for the sites 2 and 4.

understood by considering the same arguments as in Sec. III C. Namely, in order to obtain $\mathbf{P} \parallel \boldsymbol{c}$, we should consider the transfer integrals $\hat{\mathrm{t}}_{ij}$ between all possible combinations of sites i and j along $\boldsymbol{c}$. Of course, the main contribution is expected from the NN sites and, in order to contribute to $\mathbf{P} \parallel \boldsymbol{c}$, these transfer integrals should have both symmetric and antisymmetric components [see Eq. (22)]. However, due to the combination of $\{\hat{C}_c^2|\boldsymbol{c}/2\}$ and the inversion operation around the Mn sites, the NN integrals between planes $z = 0$ and $c/2$ will satisfy the following property: $\hat{R}_c^2 \hat{t}_{ij} (\hat{R}_c^2)^T = \hat{t}_{ji} = \hat{t}_{ij}^T$, where $\hat{R}_c^2$ is the 180° rotation around $\boldsymbol{c}$ in the basis of d orbitals. Thus, the effect of $\hat{R}_c^2$ is to change signs of some of the matrix elements of $\hat{t}_{ij}$. Therefore, for a given combination of orbital indices m and m', the matrix elements of $\hat{t}_{ij}$ will be either symmetric or antisymmetric. Moreover, with the proper choice of phases of the basis orbitals at the sites i and j in the CF representation, the matrix $\hat{\mathrm{t}}_{ij}$ can be made totally symmetric. Another difference from the $\boldsymbol{ab}$ plane is that the occupied e_g orbitals are nearly parallel along the $\boldsymbol{c}$ axis (the so-called "ferro-OO"). Therefore, there is no orbital alternation, which would lead to an additional asymmetry of $\hat{\mathrm{t}}_{ij}$ in the CF representation. Thus, in the second order of $1/\Delta$, the NN contributions to $\mathbf{P} \parallel \boldsymbol{c}$ will vanish, and $\mathbf{P} \parallel \boldsymbol{c}$ is finite due to either next-NN integrals, which are small, or the higher-order effects with respect to $1/\Delta$, which are also small. This naturally explains the fact that $\mathbf{P} \parallel \boldsymbol{c}$ is much smaller than $\mathbf{P} \parallel \boldsymbol{a}$.

This finding resembles behavior of $\mathbf{P}$ in nearly fourfold periodic compounds.[2,3] For example, in $TbMnO_3$ the polarization is aligned along $\boldsymbol{c}$. However, the external magnetic field along $\boldsymbol{b}$ changes the magnetic texture and realigns $\mathbf{P}$ parallel to $\boldsymbol{a}$.[3] Moreover, most of experimental data confirm that $\mathbf{P} \parallel \boldsymbol{c}$ is smaller than $\mathbf{P} \parallel \boldsymbol{a}$. For example, such a behavior is typical for the $Eu_{1-x}Y_xMnO_3$ compounds, composed from nonmagnetic rare-earth elements.[2,39] The results of this section suggest that this behavior is more generic and can be anticipated in other regimes, including twofold periodic magnetic systems. The origin of this phenomenon is related to the specific symmetry of the crystal (in our case, the orthorhombic $Pbnm$ symmetry) and how it is lowered by the magnetic order. It should not be confused with some general properties of the spin spiral.

The magnetic texture in Fig. 9 can be viewed as a "defected E-type AFM texture," where the "defects" are two FM bonds between the planes $z = 0$ and $c/2$. Of course, such "defects" are energetically unfavorable and, after including the SO interaction, this magnetic texture will change in order to minimize the FM coupling in the defected bonds. This will lead to a substantial deformation of the magnetic texture. Nevertheless, we would like to emphasize that the noncollinear magnetic texture with $\mathbf{P} \parallel \boldsymbol{c}$ can be stabilized even after including the SO interaction. The situation was discussed in Ref. 9.

IV. DISCUSSIONS AND CONCLUSIONS

This work is a continuation of previous studies, devoted to improper FE activity in orthorhombic manganites.[9,10] Our main motivation was to present a transparent physical picture, which would explain why and how the FE polarization is induced by some complex magnetic order. For these purposes, we invoke the DE theory, which was formulated for the low-energy model, derived from the first-principles electronic-structure calculations. As far as the electronic polarization is concerned, the DE theory is very robust and reproduces results of more general mean-field HF calculations at a good quantitative level. Furthermore, the main advantage of the DE theory is that it allows us to greatly simplify the problem and, in a number of cases, derive an analytical expression for the FE polarization. Thus, we could clarify very basic aspects of improper FE activity in manganites with the twofold periodic magnetic texture.

In our analysis, we started from the general Berry-phase theory.[12,13] In the case of improper ferroelectrics, the basic quantity to be considered is the electronic polarization, which incorporates the change of the electronic structure in response to the noncentrosymmetric alignment of spins. Then, our main message is that, for the analysis of electronic polarization in manganites, one can always use two physical limits. The first one is the limit of large intra-atomic splitting Δ_{ex} between majority- and minority-spin states. The second one is the limit of large intra-atomic splitting Δ between the majority-spin e_g states. Therefore, for the electronic polarization, one can always consider the perturbation-theory expansion with respect to both $1/\Delta_{ex}$ and $1/\Delta$. This perturbation theory describes asymmetric transfer of some weight of the Wannier functions to the neighboring sites, which gives rise to the polarization.

There is some similarity with the theory of superexchange interactions, which deals with the virtual hoppings,[15] and where the terms proportional to $1/\Delta$ and $1/\Delta_{ex}$ account for the FM and AFM contributions, respectively.[16] Therefore, the DE limit $\Delta_{ex} \to \infty$ would correspond to neglecting all AFM contributions. It may not be a good approximation for

interatomic magnetic interactions. Nevertheless, the main difference of polarization is that it appears only in the second order with respect to $1/\Delta$ and $1/\Delta_{ex}$. The physically relevant situation corresponds to the inequality $\Delta_{ex} > \Delta$. Then, since $(\Delta/\Delta_{ex})^2 < \Delta/\Delta_{ex}$, it is logical to keep the effects of the first order in $1/\Delta_{ex}$ for the superexchange interactions, but neglect the effects of the second order in $1/\Delta_{ex}$ for the polarization. This again justifies the use of the DE limit in the latter case.

On the basis of this perturbation-theory expansion, we were able to explain how the electronic polarization depends on the relative directions of spins in an arbitrary twofold periodic magnetic texture. Particularly, the multiferroicity in orthorhombic manganites is a nonlocal phenomenon in the sense that the inversion symmetry is broken by making some of the Mn-Mn bonds magnetically inequivalent. In the DE model, this inequivalence is achieved by additional modulation of the transfer integrals with ξ_{ij}. Then, one trivial conclusion is that there is no magnetic inversion symmetry breaking in the spin-spiral phase, where all ξ_{ij} are the same. Therefore, in order to make finite polarization, it is essential to deform the spin spiral. In orthorhombic manganites, such deformation is caused by relativistic SO interaction.[9,10] The second important precondition for the FE activity is the asymmetry of transfer integrals in the CF representation, which should have simultaneously symmetric and antisymmetric components. The main contribution to this asymmetry comes from the antiferro-OO in the ***ab*** plane. Thus, the FE polarization in orthorhombic manganites is the joint effect of spatially inhomogeneous magnetic texture and antiferro-OO, which supports the main conclusion of Ref. 20.

We also pointed out a serious problem in the structural optimization, which apparently exists in first-principles calculations (at least, at the level of LDA + U approximation for the exchange-correlation functional without SO coupling) and which typically results in large overestimation of FE polarization in comparison with experimental data.[10] In this work, we were able to clarify the origin of this problem: in theoretical structure, the directions of noncentrosymmetric atomic displacements are inconsistent with the type of the OO in the FM zigzag chains, yielding the same directions of ionic and electronic polarizations. In the experimental structure, however, these two terms have opposite directions and partially cancel each other.

Finally, we explained how the electronic polarization can be switched between orthorhombic ***a*** and ***c*** directions by inverting the magnetic texture in every second ***ab*** plane. We also expect a gigantic change of the polarization itself, which is related to very different symmetry properties of transfer integrals and OO along the ***c*** direction and in the ***ab*** plane of manganites.

In this work, our analysis was limited by twofold periodic magnetic textures, which illustrate the basic idea of the DE theory of FE polarization. The idea can be extended to the systems with more general magnetic periodicity: apart from the additional complexity of the magnetic texture, there is no fundamental difference between twofold and more general magnetic periodicity. In both cases, the basic property, which should be considered and which gives rise to the FE activity, is the alternation of angles between spins in different Mn-Mn bonds in the background of antiferro-OO.

ACKNOWLEDGMENT

This work is partly supported by a grant of the Ministry of Education and Science of Russia (Grant No. 14.A18.21.0889).

*solovyev.igor@nims.go.jp

[1] Y. Tokura, Science **312**, 1481 (2006); T. Kimura, Annu. Rev. Mater. Res. **37**, 387 (2007); S.-W. Cheong and M. Mostovoy, Nat. Mater. **6**, 13 (2007); D. Khomskii, Physics **2**, 20 (2009).

[2] S. Ishiwata, Y. Kaneko, Y. Tokunaga, Y. Taguchi, T.-h. Arima, and Y. Tokura, Phys. Rev. B **81**, 100411(R) (2010).

[3] T. Kimura, T. Goto, H. Shintani, K. Ishizaka, T. Arima, and Y. Tokura, Nature (London) **426**, 55 (2003); T. Kimura, G. Lawes, T. Goto, Y. Tokura, and A. P. Ramirez, Phys. Rev. B **71**, 224425 (2005).

[4] I. A. Sergienko, C. Şen, and E. Dagotto, Phys. Rev. Lett. **97**, 227204 (2006).

[5] S. Picozzi, K. Yamauchi, B. Sanyal, I. A. Sergienko, and E. Dagotto, Phys. Rev. Lett. **99**, 227201 (2007).

[6] H. Katsura, N. Nagaosa, and A. V. Balatsky, Phys. Rev. Lett. **95**, 057205 (2005).

[7] M. Mostovoy, Phys. Rev. Lett. **96**, 067601 (2006).

[8] I. A. Sergienko and E. Dagotto, Phys. Rev. B **73**, 094434 (2006).

[9] I. V. Solovyev, Phys. Rev. B **83**, 054404 (2011).

[10] I. V. Solovyev, M. V. Valentyuk, and V. V. Mazurenko, Phys. Rev. B **86**, 144406 (2012).

[11] M. Mochizuki, N. Furukawa, and N. Nagaosa, Phys. Rev. Lett. **105**, 037205 (2010).

[12] R. D. King-Smith and D. Vanderbilt, Phys. Rev. B **47**, 1651 (1993); D. Vanderbilt and R. D. King-Smith, *ibid.* **48**, 4442 (1993).

[13] R. Resta, J. Phys.: Condens. Matter **22**, 123201 (2010).

[14] K. Yamauchi, F. Freimuth, S. Blügel, and S. Picozzi, Phys. Rev. B **78**, 014403 (2008).

[15] P. W. Anderson, Phys. Rev. **115**, 2 (1959).

[16] K. I. Kugel and D. I. Khomskii, Usp. Fiz. Nauk **136**, 621 (1982) [Sov. Phys. Usp. **25**, 231 (1982)].

[17] E. J. Mele and P. Král, Phys. Rev. Lett. **88**, 056803 (2002).

[18] I. V. Solovyev and Z. V. Pchelkina, Phys. Rev. B **82**, 094425 (2010).

[19] P. Barone, S. Picozzi, and J. van den Brink, Phys. Rev. B **83**, 233103 (2011); P. Barone and S. Picozzi, *ibid.* **85**, 214101 (2012).

[20] P. Barone, K. Yamauchi, and S. Picozzi, Phys. Rev. Lett. **106**, 077201 (2011).

[21] D. Okuyama, S. Ishiwata, Y. Takahashi, K. Yamauchi, S. Picozzi, K. Sugimoto, H. Sakai, M. Takata, R. Shimano, Y. Taguchi, T. Arima, and Y. Tokura, Phys. Rev. B **84**, 054440 (2011).

[22] C. Zener, Phys. Rev. **82**, 440 (1951); P. W. Anderson and H. Hasegawa, *ibid.* **100**, 675 (1955); P.-G. de Gennes, *ibid.* **118**, 141 (1960); K. Kubo and N. Ohata, J. Phys. Soc. Jpn. **33**, 21 (1972).

[23] Recent developments on the DE model and its generalizations in the context of colossal magnetoresistant manganites can be found, e.g., in E. Dagotto, T. Hotta, and A. Moreo, Phys. Rep. **344**, 1 (2001).

[24] I. V. Solovyev, J. Phys.: Condens. Matter **20**, 293201 (2008).

[25] I. Solovyev, J. Phys. Soc. Jpn. **78**, 054710 (2009).

[26]I. V. Solovyev and K. Terakura, Phys. Rev. Lett. **83**, 2825 (1999); I. V. Solovyev, Phys. Rev. B **63**, 174406 (2001).
[27]J. Kanamori, J. Appl. Phys. **31**, 14S (1960).
[28]J. C. Slater and G. F. Koster, Phys. Rev. **94**, 1498 (1954).
[29]X. L. Qi, T. L. Hughes, and S.-C. Zhang, Phys. Rev. B **78**, 195424 (2008).
[30]T. Hotta, M. Moraghebi, A. Feiguin, A. Moreo, S. Yunoki, and E. Dagotto, Phys. Rev. Lett. **90**, 247203 (2003).
[31]For $\Delta = 0$, the integral (15) can be evaluated analytically: note that $\int_0^{2\pi/a} dk = \int_0^{\pi/a} dk + \int_{\pi/a}^{2\pi/a} dk$, and use that $\int_{\pi/a}^{2\pi/a} dk$ can be further transformed to $\int_0^{\pi/a} dk$ after replacing $d_z(k)$ by $-d_z(k)$.
[32]J. Zak, Phys. Rev. Lett. **62**, 2747 (1989).
[33]Note also the difference in definition of the model parameters: Δ in our work corresponds to $E_{\rm JT}$ multiplied by normal modes of vibration, which are found self-consistently in Ref. 20. Thus, in terms of $E_{\rm JT}$, the OO and FE polarizations develop starting only from some critical value.
[34]A. Muñoz, M. T. Casáis, J. A. Alonso, M. J. Martínez-Lope, J. L. Martínez, and M. T. Fernández-Díaz, Inorg. Chem. **40**, 1020 (2001).
[35]The fitting error can be defined as $I = \frac{1}{2}[\sum_{mm'}(\mathfrak{t}_{12}^{mm'} - \tilde{\mathfrak{t}}_{12}^{mm'})^2]^{1/2}$, where $\mathfrak{t}_{12}^{mm'}$ and $\tilde{\mathfrak{t}}_{12}^{mm'}$ are the original and fitted matrix elements, respectively. Then, the best fitting ($I = 3$ meV) is obtained for the $+U$ parameters of YMO ($P2_1nm$, LSDA), where β is found to be the closest to 60°. The worst fitting ($I = 23$ meV) is obtained for bare LDA parameters of HMO, having largest deviation from $\beta = 60°$.
[36]J. He and C. Franchini, Phys. Rev. B **86**, 235117 (2012).
[37]A. Stroppa and S. Picozzi, Phys. Chem. Chem. Phys. **12**, 5405 (2010).
[38]A. Malashevich and D. Vanderbilt, Phys. Rev. Lett. **101**, 037210 (2008); Phys. Rev. B **80**, 224407 (2009).
[39]K. Noda, M. Akaki, F. Nakamura, D. Akahoshi, and H. Kuwahara, J. Magn. Magn. Mater. **310**, 1162 (2007).